jove

Analysis of Somatic Hypermutation in the JH4 intron of Germinal Center B cells from Mouse Peyer's Patches

Emily Sible[1], **Simin Zheng**[2], **Jee Eun Choi**[1], **Bao Q. Vuong**[1]

[1] Department of Biology, The City College of New York and The Graduate Center of The City University of New York [2] Department of Microbiology, Icahn School of Medicine at Mount Sinai

Corresponding Author

Bao Q. Vuong
bvuong@ccny.cuny.edu

Citation

Sible, E., Zheng, S., Choi, J.E., Vuong, B.Q. Analysis of Somatic Hypermutation in the JH4 intron of Germinal Center B cells from Mouse Peyer's Patches. *J. Vis. Exp.* (170), e61551, doi:10.3791/61551 (2021).

Date Published

April 20, 2021

DOI

10.3791/61551

URL

jove.com/video/61551

Abstract

Within the germinal centers of lymphoid organs, mature B cells alter their expressed immunoglobulin (Ig) by introducing untemplated mutations into the variable coding exons of the Ig heavy and light chain gene loci. This process of somatic hypermutation (SHM) requires the enzyme activation-induced cytidine deaminase (AID), which converts deoxycytidines (C), into deoxyuridines (U). Processing the AID-generated U:G mismatches into mutations by the base excision and mismatch repair pathways introduces new Ig coding sequences that may produce a higher affinity Ig. Mutations in *AID* or DNA repair genes can block or significantly alter the types of mutations observed in the Ig loci. We describe a protocol to quantify JH4 intron mutations that uses fluorescence activated cell sorting (FACS), PCR, and Sanger sequencing. Although this assay does not directly measure Ig affinity maturation, it is indicative of mutations in Ig variable coding sequences. Additionally, these methods utilize common molecular biology techniques which analyze mutations in Ig sequences of multiple B cell clones. Thus, this assay is an invaluable tool in the study of SHM and Ig diversification.

Introduction

B cells, members of the adaptive immune system, recognize and eliminate antigens by producing antibodies, also known as immunoglobulins (Ig). Each Ig is composed of two heavy (IgH) and two light (IgL) chain polypeptides, which are held together by disulfide bonds to form the characteristic “Y” shape structure of the Ig[1]. The N-termini of IgH and IgL comprise the variable (V) region of each polypeptide and together they form the antigen binding site of the Ig, whereas the constant region of IgH imparts the effector function of the Ig. Developing B cells in the bone marrow rearrange the V coding exons of IgH and IgL in a process known as V(D)J recombination[2,3,4]. Transcription of the recombined V exons, coupled with the respective constant region exons, forms the mRNA that is translated into the Ig.

Mature B cells expressing a membrane bound Ig, also known as a B cell receptor (BCR), circulate to secondary

Copyright © 2021 JoVE Creative Commons Attribution-NonCommercial-NoDerivs 3.0 Unported License

lymphoid organs, such as the spleen, lymph node, or Peyer's patches, where they survey the environment for antigens and interact with other cells of the immune system[1]. Within the germinal centers (GC) of secondary lymphoid organs, B cells that recognize antigen through the BCR become activated. Aided by follicular dendritic cells and follicular helper T cells, activated B cells can then proliferate and differentiate into plasma and memory cells, which are important effectors of a robust immune response[5,6,7,8,9]. Additionally, these activated B cells can undergo secondary Ig gene diversification processes - class switch recombination (CSR) and somatic hypermutation (SHM). During CSR, B cells exchange the default μ constant region of the IgH polypeptide with another constant region (γ, α, ε) through a DNA deletional-recombination reaction (**Figure 1**). This allows for the expression of a different constant exon and translation of a new Ig. The B cell will switch from expressing IgM to another isotype (IgG, IgA, IgE). CSR changes the effector function of the Ig without altering its antigen specificity[10,11,12]. However, during SHM, B cells mutate the V coding regions of IgH and IgL to enable the production and selection of higher affinity Igs, which can more effectively eliminate an antigen[13,14,15] (**Figure 1**). Importantly, both CSR and SHM depend on the function of one enzyme: activation-induced cytidine deaminase (AID)[16,17,18]. Humans and mice deficient in AID cannot complete CSR or SHM and present with elevated IgM serum titers or Hyper-IgM[17,19].

In CSR, AID deaminates deoxycytidines (C) in the repetitive switch regions that precede each constant coding exons, converting them into deoxyuridines (U)[20,21], which creates mismatched base pairing between deoxyuridines and deoxyguanosines (U:G). These U:G mismatches are converted into the double-stranded DNA breaks, which are required for DNA recombination, by either the base excision repair (BER) or mismatch repair (MMR) pathway[22,23,24,25,26,27,28,29]. In SHM, AID deaminates C within the V coding exons. Replication across the U:G mismatch generates C:G to T:A transition mutations, whereas removal of the uracil base by the BER protein, uracil DNA glycosylase (UNG), prior to DNA replication produces both transition and transversion mutations[16]. Null mutations in *UNG* significantly increase C:G to T:A transition mutations[21,22]. Similar to CSR, SHM requires the complementary roles of MMR and BER. During SHM, MMR generates mutations at A:T base pairs. Inactivating mutations in MutS homology 2 (*MSH2*) or DNA polymerase η (*Polη*) significantly reduces mutations at A:T bases and compound mutations in *MSH2* and *Polη* virtually abolishes mutations at A:T bases[21,30,31]. Consistent with the critical role for BER and MMR in converting AID-generated U into transition or transversion mutations, mice deficient for both MSH2 and UNG (*MSH2*$^{-/-}$ *UNG*$^{-/-}$) display only C:G to T:A transition mutations resulting from replication across the U:G mismatch[21].

The analysis of SHM in V coding regions remains complicated because developing B cells can recombine any of the V(D)J coding exons in the *IgH* and *IgL* loci[1,2,4]. Accurate analysis of these uniquely recombined and somatically mutated V regions requires the identification and isolation of clones of B cells or the Ig mRNA[11,13]. The JH4 intron, which is 3' of the last J coding exon in the IgH locus, harbors somatic mutations due to the spreading of mutations 3' of the V promoter[32,33,34] and therefore is frequently used as a surrogate marker for SHM in V regions[31,35] (**Figure 1**). To experimentally elucidate how specific genes or genetic mutations alter SHM patterns or rates, the JH4 intron can be sequenced from Peyer's patches (PP) germinal center B cells (GCBCs),

Copyright © 2021 JoVE Creative Commons Attribution-NonCommercial-NoDerivs 3.0 Unported License

which undergo high rates of SHM[36,37,38]. GCBCs can be readily identified and isolated with fluorescently conjugated antibodies against cell surface markers ($B220^+PNA^{HI}$)[17,39].

A detailed protocol is presented to characterize JH4 intron mutations in PP GCBCs from mice using a combination of FACS (fluorescence activated cell sorting), PCR, and Sanger sequencing (**Figure 2**).

Protocol

All mutant mice were maintained on a C57BL/6 background. Age-matched (2-5 months old) male and female mice were used for all experiments. Husbandry of and experiments with mice were conducted according to protocols approved by The City College of New York Institutional Animal Care and Use Committee.

1. Dissection of Peyer's patches

1. Euthanize the mouse with 100% CO_2 at 3 L/min for 5 min followed by cervical dislocation to confirm death. Sterilize dissection tools (scissors, forceps, fine forceps) and gloved hands with 70% ethanol.
2. Lay the mouse on the dissection pad with the abdomen exposed. Generously spray the body of the mouse with 70% ethanol prior to making any incisions to sterilize the dissection area.
3. Make an incision into the skin across the abdomen and remove the skin from the abdomen by pulling simultaneously on both sides of the incision towards the head and tail using forceps (or sterilized, gloved hands).
4. Pin down the fore and hind limbs of the mouse.
5. Cut the peritoneal cavity with scissors to expose the internal organs.
6. Locate the small intestine between the stomach and caecum ("J" shaped structure near the colon). Remove the small intestine by cutting below the stomach and above the caecum.
7. Remove any connective tissue and fat linking the folds of the small intestine together.
   NOTE: Fat will have a distinctive white color, unlike the pink color of the small intestine.
8. Examine the external surface of the small intestine for the Peyer's patches (PPs), which are small (~1 mm), oval-shaped structures that appear white below a thin layer of translucent epithelial cells.
9. Carefully excise all visible PP with scissors.
   NOTE: One C57BL/6 wild-type (WT) mouse can yield 4-8 PPs, whereas an *AID*$^{-/-}$ mouse will have 6-10 PPs.
10. Collect the PPs into a 1.5 mL microcentrifuge tube containing 1 mL of FACS buffer on ice.
    NOTE: The PP should sink, whereas fat will float to the surface and can be removed.

2. Cell isolation for FACS

1. Place a 40 µm filter in a 6-well dish with 1 mL of cold (4 °C) FACS buffer.
2. Pour the PPs from the 1.5 mL tube onto the filter.
3. Wash PPs with 1 mL of cold FACS buffer, making sure that they are always in liquid and on ice.
4. Use the flat end of the plunger from a 1 mL syringe as a pestle to crush the PPs on the filter until only connective tissue remains on the filter.
5. Wash the filter and plunger with 1 mL of cold FACS buffer to release the cells into the 6 well dish.

Copyright © 2021 JoVE Creative Commons Attribution-NonCommercial-NoDerivs 3.0 Unported License

6. Collect the ~4 mL of cells in cold FACS buffer and filter them through a 40 µm strainer cap FACS tube.
7. Wash the strainer cap with 1 mL of cold FACS buffer.
8. Pellet the cells at 600 *x g* at 4 °C for 5 min in a swinging bucket centrifuge.
9. Decant the supernatant.
10. Resuspend the cells in 0.4 mL of cold FACS buffer.
11. Remove 10 µL for cell counting to verify yield (expect ~5 x 10^6 cells/mouse, see **Figure 3A**)
12. Filter the remaining cells through a 40 µm strainer cap into a FACS tube and proceed to staining for FACS.

3. Staining GCBCs for FACS

1. Add 1 µL Fc block (unlabeled anti-mouse CD16/CD32) to the 400 µL cell suspension and place the cells on ice for 15 min.
2. Add 2 mL of cold FACS buffer to wash the cells.
    1. Pellet cells at 600 *x g* at 4 °C for 5 min and discard the supernatant.
3. Resuspend the cells in 80 µL of cold FACS buffer.
4. Remove 10 µL of cells from the WT PP for each staining control (4 in total, including 3 single stain controls and 1 unstained control). Leave 40 µL of the WT PP for the next step. Alternatively, use compensation beads for the staining controls.
5. Stain each of the experimental samples (e.g., WT and *AID*$^{-/-}$) in 500 µL of cold FACS buffer with 2.5 µL of peanut agglutinin (PNA)-biotin for 15 min on ice.
6. Add 2 mL of cold FACS buffer to wash the cells.
    1. Pellet cells at 600 *x g* at 4 °C for 5 min and discard the supernatant.
7. Stain each experimental sample with 500 µL of the cocktail in the dark, on ice, for 15 min **(Table 1).** Ensure the cells are fully resuspended in the staining cocktail.
8. Prepare single stain controls for the compensation matrix.
    1. Stain the cells in 500 µL of cold FACS buffer using the dilutions specified in **Table 2**.
    2. Incubate the staining controls in the dark, on ice, for 15 min.
9. Add 2 mL cold FACS buffer to all the tubes in steps 3.7 and 3.8, pellet the cells, and discard the supernatant to wash off unbound antibodies or DAPI.
10. Resuspend the cells in 500 µL of cold FACS buffer and place on ice.
11. Using a cell sorter, collect $B220^+PNA^{HI}$ from each stained experimental sample. **Figure 3B** shows the typical percentages of $B220^+$ PNA^{HI} obtained from WT and *AID*$^{-/-}$ PPs. **Figure 3C** displays the FACS gating strategy.

4. DNA extraction from GCBCs

1. Pellet sorted cells at 600 *x g* at 4 °C for 5 min and discard the supernatant.
2. Resuspend the cells in 1 mL of cold FACS buffer and transfer the cells into a 1.5 mL microcentrifuge tube.
    1. Pellet the cells at 600 *x g* at 4 °C for 5 min and discard the supernatant.
3. Resuspend the cells in 500 µL of DNA extraction buffer and 5 µL of 20 mg/mL Proteinase K.

Copyright © 2021 JoVE Creative Commons Attribution-NonCommercial-NoDerivs 3.0 Unported License

4. Incubate at 56 °C overnight.
5. Precipitate DNA with 500 µL isopropanol and 1 µL of 20 mg/mL glycogen. Mix the tube thoroughly by inverting 5-6x.
6. Incubate at room temperature for 10 min.
7. Centrifuge in a microcentrifuge for 15 min at 25 °C at 21,000 *x g*.
    1. Discard the supernatant and retain the pellet, which contains the precipitated DNA and glycogen.
8. Wash the DNA pellet with 1 mL of 70% ethanol.
    1. Pellet the DNA in a microcentrifuge for 10 min at 25 °C at 21,000 *x g*.
    2. Remove the 70% ethanol and air-dry the DNA pellet for 5-10 min.
    NOTE: Avoid over-drying as the DNA may not rehydrate completely.
9. Resuspend the DNA in 30 µL TE buffer and incubate overnight at 56 °C.

5. JH4 intron sequence amplification and analysis

1. Quantify DNA by measuring the absorbance at a wavelength of 260 nm (A260).
NOTE: The typical concentration of DNA recovered from sorted $B220^{+}PNA^{HI}$ GCBCs of a C57BL/6 mouse is 20-40 ng/µL.
2. Perform the nested PCR for the JH4 intron (**Table 3, Table 4**). Normalize the total amount of genomic DNA used in the first PCR to the least concentrated sample. (e.g., if the least concentrated sample is 5 ng/µL, use 58.75 ng of DNA for all the samples in the maximum volume of water (11.75 µL) in PCR #1).
3. Resolve the PCR product on a 1.5% agarose gel at 200 V for 20 min. The expected amplicon size is 580 bp.
4. Excise the amplicon from the gel and extract the DNA using a gel extraction kit according to manufacturer's instructions (see **Supplementary Figure 1**).
    1. Elute the DNA with 30 µL of water and quantify the amount of DNA by measuring the A260.
    NOTE: The typical concentration of the purified PCR product is 3-10 ng/µL.
5. Ligate the purified PCR product into a plasmid with blunt ends. Standardize the total amount of PCR product used in every ligation reaction (**Table 5**).
    1. Incubate the ligation reaction at room temperature for 5 min or overnight at 16 °C.
6. Transform electrocompetent bacterial cells with 2 µL of the ligation reaction.
    1. Electroporate at 1.65 kV.
    2. Rescue in 600 µL of SOC media for 1 h at 37 °C in a shaking incubator at 225 rpm.
    3. Plate 100 µL of transformed bacteria onto LB supplemented with ampicillin (100 µg/mL) agar plates and incubate overnight at 37 °C.
7. Submit the plate of bacterial colonies for Sanger sequencing using the T7 forward primer. Alternatively, grow overnight cultures of each bacterial colony and perform a plasmid purification.
    1. If necessary, repeat the PCR, ligation, and/or transformation to optimize the yield of bacterial colonies
    NOTE: A minimum of 30 colonies should be picked from each plate.

Copyright © 2021 JoVE Creative Commons Attribution-NonCommercial-NoDerivs 3.0 Unported License

8. Standardize the sequence data in the .txt files
    1. Delete the plasmid sequence.
    2. Ensure every sequence is oriented 5' to 3' according to the JH4 intron reference sequence (NG_005838). Generate the reverse complement of any sequence, as necessary.
9. Align the sequences obtained for each PCR against the JH4 intron reference sequence (NG_005838) using a Clustal Omega software (**Figure 4A**).
    1. Identify differences from the reference sequence as mutations
    2. Verify that all mutations are true point mutations by examining the electropherogram of the Sanger sequencing. Repeat sequencing if necessary. (**Figure 4B,C**).
10. Tabulate and quantify unique mutations in the JH4 intron for each genotype (**Figure 5**).
    1. Count sequences with identical mutations only once
    NOTE: It is not possible to determine if the identical sequences were generated during the PCR or identical SHM events in different B cells.
    2. Count every instance of WT germline JH4 intron sequences (i.e., those with no mutations) as a unique sequence.

Representative Results

Flow cytometry

Mature B cells circulate to germinal centers where they undergo affinity maturation, clonal expansion, and differentiation into plasma or memory cells[40,41,42,43,44]. These GCBCs can be identified by numerous cell surface markers, including high expression of the CD45R/B220 receptor and binding of peanut agglutinin (PNA)[45,46]. To isolate activated GCBCs, PP cells were stained with anti-B220 antibodies conjugated to phycoerythrin (PE) and biotinylated-PNA, followed by streptavidin conjugated to APC-eFluor780. Dead cells were eliminated using the fluorescent 4',6-Diamidino-2-Phenylindole (DAPI) dye, which stains the nucleic acid of dying or dead cells[47,48]. The stained cells were subsequently analyzed and sorted via flow cytometry. The PPs consisted of ~80% $B220^+$ cells[49,50]. WT PPs contain on an average 4 x 10^6 cells per mouse (**Figure 3A**). Approximately 8% of the WT PP cells were $B220^+PNA^{HI}$, which is half the number observed in *AID*$^{-/-}$ (**Figure 3B**). Thus, 0.3-0.6 x 10^6 $B220^+PNA^{HI}$ GCBCs were obtained after sorting, which were sufficient to analyze mutations in the JH4 intron.

JH4 Sequence Analysis

The JH4 intron was amplified by a nested PCR using common VHJ558 family primers (J558FR3Fw and VHJ558.2) followed by JH4 intron spanning primers VHJ558.3 and VHJ558.4[35,37]. Of the 105 unique sequences obtained from WT GCBCs, a total of 226 mutations were found (**Figure 5A**). Analysis of the GCBC mutation spectrum in the WT mice showed a range of transitions and transversions at a rate of 4 x 10^{-3} mutations/bp, which was calculated by dividing the total number of mutated bases by the total number of bases that were sequenced[32,36,37,38]. Additionally, each JH4 PCR product from WT GCBCs contained 1-25 mutations (**Figure 5B**), where multiple mutations were frequently found on one sequence[33,36]. Only two mutations were identified in 113 *AID*$^{-/-}$ sequences (**Figure 5A**). *AID*$^{-/-}$ B cells exhibited 1.66 x 10^{-5} mutations/bp, which was significantly lower than WT B cells ($p < 0.05$)[36] and compares to the error rate of the high fidelity polymerase (5.3 x 10^{-7} sub/base/doubling)[51,52].

Copyright © 2021 JoVE Creative Commons Attribution-NonCommercial-NoDerivs 3.0 Unported License

Thus, *AID*$^{-/-}$ B cells served as a useful negative control for this assay.

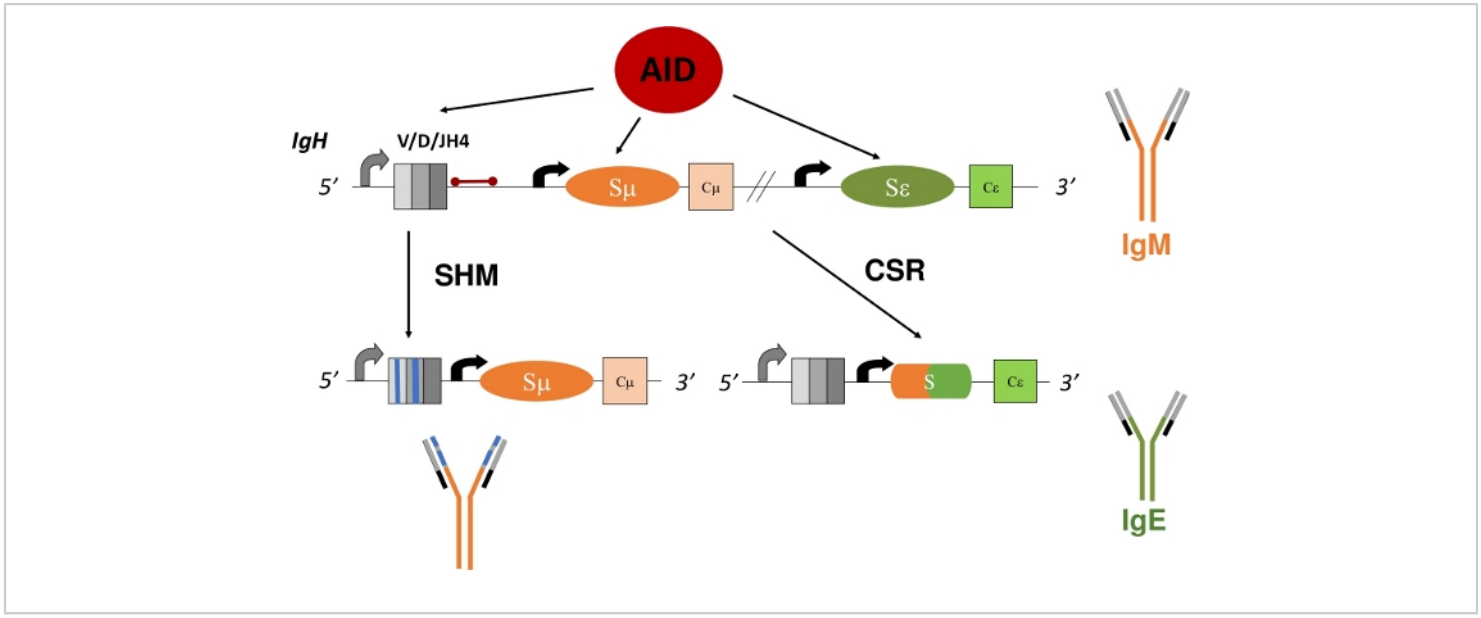

Figure 1: Schematic of the *IgH* gene locus and the regions targeted by AID during CSR and SHM. The red bar indicates the 580 bp JH4 intron that is 3' of VDJH4 rearrangements and is analyzed in this protocol. In CSR, AID-dependent deamination of intronic switch regions (Sμ and Sε) promotes DSB formation that allows for deletional-recombination and the expression of a new antibody isotype (IgM to IgE). During SHM, V regions (grey boxes) accumulate mutations (blue lines) that may lead to higher affinity Ig. Please click here to view a larger version of this figure.

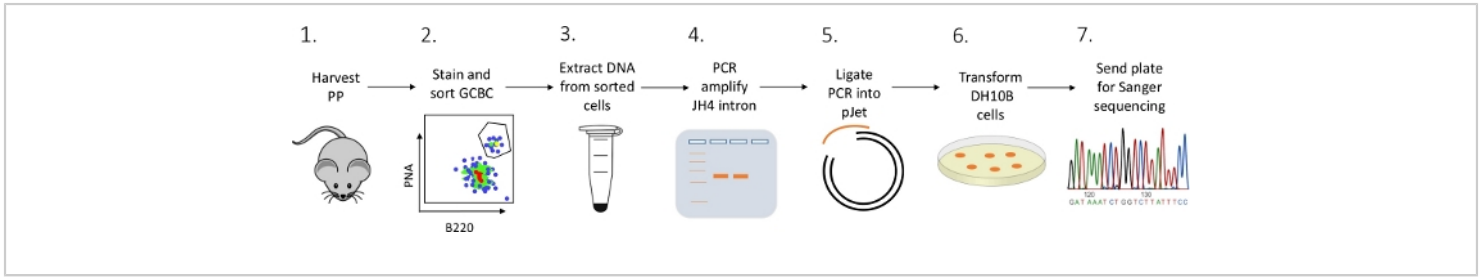

Figure 2: Workflow to analyze SHM of the JH4 intron in GCBCs isolated from PPs. Please click here to view a larger version of this figure.

Copyright © 2021 JoVE Creative Commons Attribution-NonCommercial-NoDerivs 3.0 Unported License

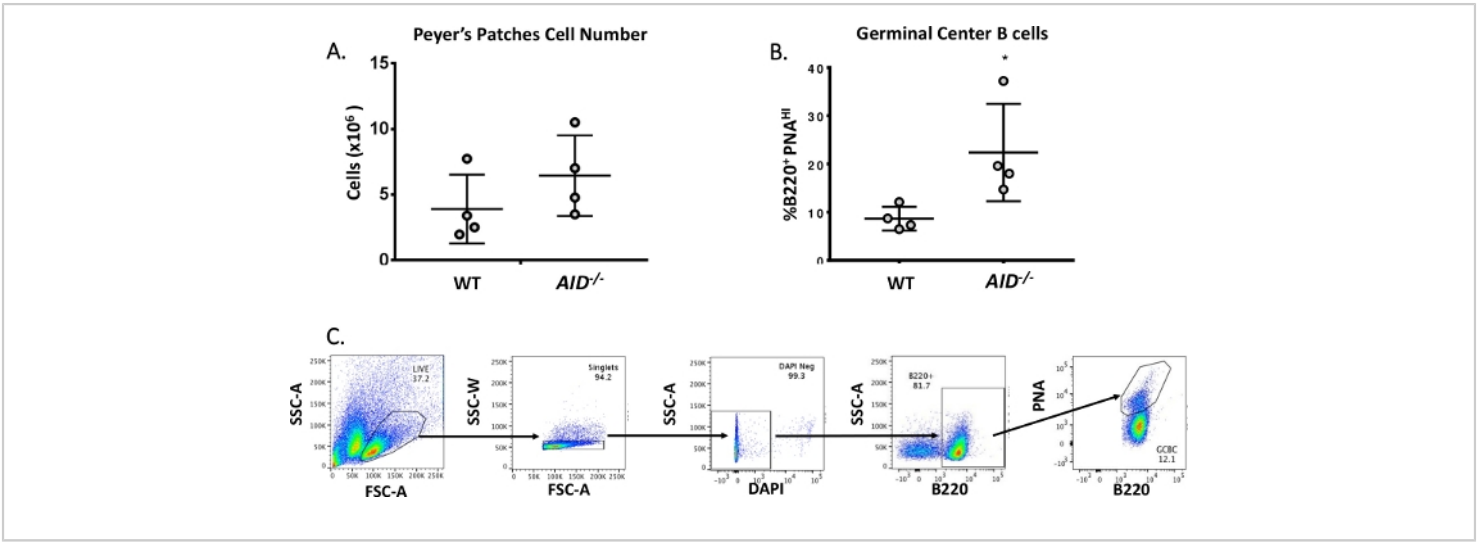

Figure 3: Characterization of PP GCBCs. (**A**) Total number of PP cells from WT and *AID*$^{-/-}$ mice (n = 4 per genotype). Error bars represent standard deviation from the mean. (**B**) Percentage of B220^{+}PNA^{HI} GCBCs obtained from PPs of WT and *AID*$^{-/-}$ mice (n = 4 per genotype)[36]. Error bars represent standard deviation from the mean, *p<0.05 using student's t-test. (**C**) Representative FACS plots to sort B220^{+}PNA^{HI} GCBCs from PPs. Please click here to view a larger version of this figure.

Copyright © 2021 JoVE Creative Commons Attribution-NonCommercial-NoDerivs 3.0 Unported License

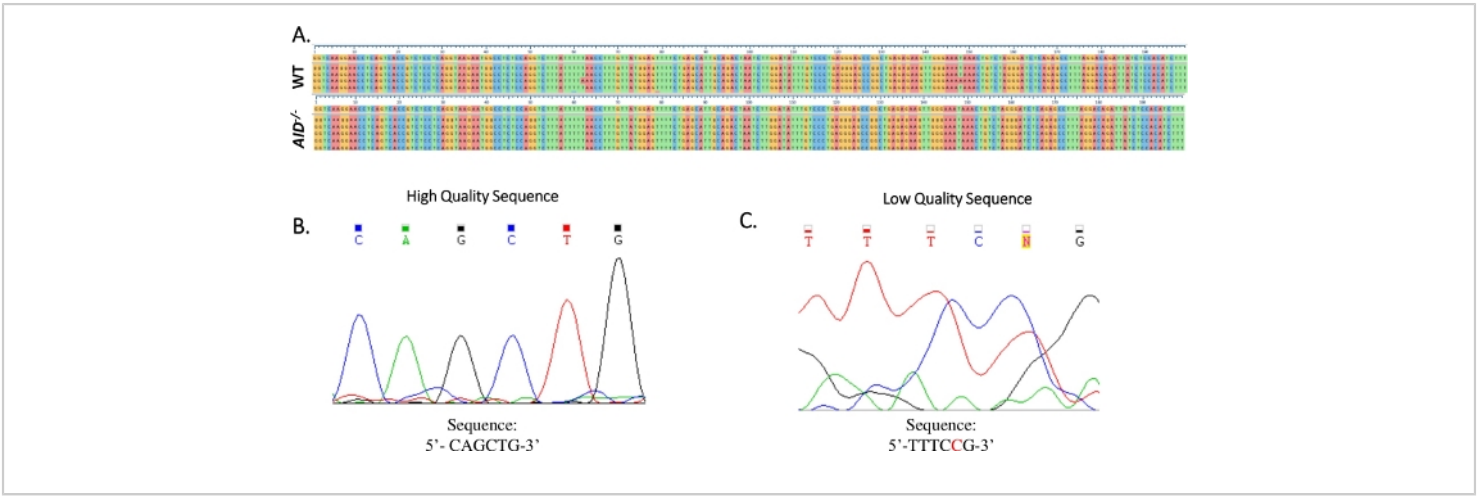

Figure 4: Analysis of JH4 Sanger sequence data. (**A**) Sample sequence alignments of Sanger sequence data of the JH4 PCR product from WT (top) and *AID*$^{-/-}$ (bottom) GCBCs to the reference genomic sequence (NG_005838), which is the sequence immediately below the numbered tick marks. Alignments were generated using Clustal Omega. (**B**) Electropherogram of high-quality Sanger sequence data, which displayed distinct peaks for each base. (**C**) Electropherogram of low-quality sequence data, which showed ambiguous peaks and unspecified bases (N). The nucleotide shown in red must be manually annotated in the sequence text file. Please click here to view a larger version of this figure.

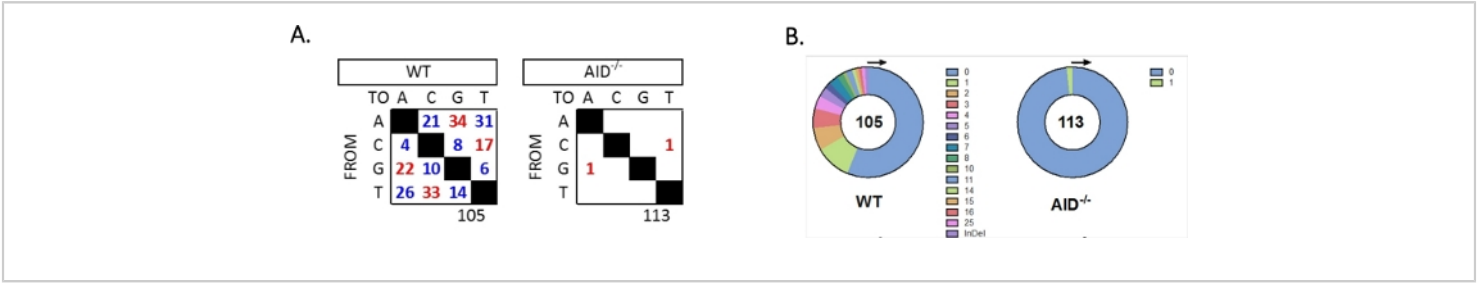

Figure 5: Analysis of mutations in the JH4 intron in WT and *AID*$^{-/-}$ GCBCs. (**A**) The total number of transition (red) and transversion (blue) mutations at A, C, G, and T bases for each genotype is summarized in the tables. The total number of sequences analyzed is indicated below the table. (**B**) The number of mutations per PCR amplicon for each genotype is depicted in the pie charts. This figure has been modified from Choi et al.[36] Copyright 2020. The American Association of Immunologists, Inc. Please click here to view a larger version of this figure.

Copyright © 2021 JoVE Creative Commons Attribution-NonCommercial-NoDerivs 3.0 Unported License

Staining Cocktail for GCBCs		Volume: 500 µL	
Antibody or Dye	**Fluorophore**	**Dilution**	**µL**
B220	PE	1000	0.5
Streptavidin	APC-eFluor780	500	1
DAPI	*N/A*	500	1

Table 1: Staining cocktails for GCBCs. Cocktail of the indicated antibodies or dye (indicated in italics) at the specified dilutions were used to stain PP cells in 500 µL for flow cytometry.

Single Stains for Compensation		Volume: 500 µL	
Antibody or Dye	**Fluorophore**	**Dilution**	**µL**
B220	PE	1000	0.5
B220	APC-eFluor780	750	0.67
DAPI	*N/A*	500	1

Table 2: Single stain controls for compensation. B220 antibodies conjugated to the indicated fluorophores were used for single stain controls to compensate for spectral overlap.

PCR #1				
Reagent	**Volume**	**Thermocycler Conditions**		
5x Buffer	4 µL	1	95 °C	3 min
10 mM dNTP	2 µL	2	94 °C	30 sec
10 µM J558FR3Fw	1 µL	3	55 °C	30 sec
10 µM VHJ558.2	1 µL	4	72 °C	1:30 min
High Fidelity DNA polymerase	0.25 µL	Cycle 2-4 9x		

Copyright © 2021 JoVE Creative Commons Attribution-NonCommercial-NoDerivs 3.0 Unported License

DNA	x (standardize to least concentrated sample)			
H_2O	to 20 µL	5	72 °C	5 min
Dilute PCR product 1:5 in H_2O before proceeding to PCR #2				

Table 3: Nested PCR of the JH4 intron. PCR components and thermocycler conditions for the first amplification reaction. Dilute the first PCR product 1:5 with water and use 1 µL of this dilution for the second PCR.

PCR #2				
Reagent	**Volume**	**Thermocycler Conditions #2**		
5x Buffer	4 µL	1	94 °C	3 min
10 mM dNTP	2 µL	2	94 °C	30 sec
10 µM VHJ558.3	1 µL	3	55 °C	30 sec
10 µM VHJ558.4	1 µL	4	72 °C	30 sec
High Fidelity DNA polymerase	0.25 µL	Cycle 2-4 21x		
Diluted PCR#1	1 µL			
H_2O	to 20 µL	5	72 °C	5 min

Table 4: PCR components and thermocycler conditions for the second PCR.

Reagent	**Volume**
2x Buffer	10 µL
Purified PCR	x (standardize to least concentrated sample)
Plasmid with blunt ends	1 µL
T4 DNA Ligase	1 µL

Copyright © 2021 JoVE Creative Commons Attribution-NonCommercial-NoDerivs 3.0 Unported License

H_2O	to 20 µL
Incubate at room temp for 5 min or overnight at 16ºC	

Table 5: Ligation reaction. Components for the ligation of the purified JH4 intron PCR product into the plasmid.

FACS Buffer
Heat inactivate FBS at 56 ˚C for one hour prior to use. Supplement PBS, pH 7.4 (Gibco, #10010049) with 2.5% (v/v) of heat-inactivated FBS. Store at 4˚C.
DNA Extraction Buffer (100 mM Tris pH 8.0, 0.1 M EDTA, 0.5% (w/v) SDS)
Add 50 mL of 1 M Tris pH 8.0, 100mL of 0.5 M EDTA, and 12.5 mL of 20% SDS. Add distilled water to 500 mL. Store at room temperature.
TE Buffer (10 mM Tris pH 8.0, 1 mM EDTA)
Add 2.5 mL of 1 M Tris pH 8.0, and 500 mL of 0.5 M EDTA. Add distilled water to 250 mL. Store at room temperature.

Table 6: Buffer recipes.

Oligonucleotides List	
J558FR3Fw	5’-GCCTGACATCTGAGGACTCTGC-3’
VHJ558.2	5’-CTGGACTTTCGGTTTGGTG-3’
VHJ558.3	5’-GGTCAAGGAACCTCAGTCA-3’
VHJ558.4	5’-TCTCTAGACAGCAACTAC-3’

Table 7: Oligonucleotides used in the assay.

Supplementary Figure 1: Representative agarose gel image after completion of step 5.4. The JH4 intron nested PCR product was resolved on a 1.5% agarose gel and the 580 bp amplicon was excised. WT PP indicates that WT PP GCBC genomic DNA was used as a template for the first PCR and AID PP indicates that *AID*$^{-/-}$ PP GCBC genomic DNA

Copyright © 2021 JoVE Creative Commons Attribution-NonCommercial-NoDerivs 3.0 Unported License

was used as a template for the first PCR. ϕ indicates the no template PCR control and - indicates nothing was loaded into the well of the agarose gel. The last lane shows a 100 bp DNA ladder. Please click here to download this figure.

Discussion

Characterizing SHM within the *IgH* and *IgL* V coding sequences of a heterogenous B cell population presents a challenge, given that each B cell uniquely reorganizes V coding segments during V(D)J recombination[34]. In this paper, we describe a method to identify mutations in the JH4 intron of GCBCs. The JH4 intron, which is located 3' of the last J coding segment in the *IgH* locus, is used as a surrogate for SHM of V regions (**Figure 1**)[31,33,34,35]. To catalog these JH4 intron mutations and assess how specific genes affect the production or pattern of mutations, PP GCBCs are specifically analyzed. These cells accumulate JH4 intron mutations as a result of chronic stimulation by intestinal microbiota[53]. Furthermore, the $B220^{+}PNA^{HI}$ GCBCs from the PPs of unimmunized mice have a mutation spectra that compares to splenic GCBCs from immunized animals[54,55]. However, mutations in the JH4 intron cannot be correlated to Ig affinity maturation because these mutations are non-coding.

To determine whether SHM alters Ig affinity, mice should be immunized intraperitoneally with an antigen, such as NP (4-hydroxy-3-nitrophenylacetyl) conjugated to CGG (chicken gamma globulin) or KLH (keyhole limpet hemocyanin)[56]. Subsequently, mRNA can be purified from splenic $B220^{+}PNA^{HI}$ GCBCs to examine SHM within V_H186.2, the V coding exon that most frequently recognizes NP and is mutated following NP-CGG or NP-KLH immunization[31,57,58,59,60]. Mutation of tryptophan-33 to a leucine in V_H186.2 has been characterized to increase Ig affinity up to 10-fold[59,60] and is, therefore, one indicator that SHM and clonal selection has generated high affinity Ig. Measuring NP7- and NP20-specific serum Ig titers by ELISA and calculating the Ig-specific NP7/NP20 ratio during the course of the immunization also documents Ig affinity maturation resulting from SHM of V regions[17,21,36]. Both these assays can be used to correlate SHM within the V_H186.2 coding sequences with changes in NP-specific Ig affinity maturation.

Whether immunized or unimmunized animals are used to analyze SHM of V_H186.2 or the JH4 intron, GCBCs must be accurately identified. We present a FACS based approach to isolate $B220^{+}PNA^{HI}$ GCBCs. Alternatively, Fas and non-sulfated α2-6-sialyl-LacNAc antigen, which is recognized by the GL7 antibody[61,62,63,64], can also be used to isolate GCBCs, which are identified as $B220^{+}Fas^{+}GL7^{+65}$ or $CD19^{+}Fas^{+}GL7^{+37}$. GL7 expression closely mirrors PNA in activated GCBCs of the lymph nodes[64,65,66]. In addition to using antibody markers specific for GCBCs, staining cocktails should maximize the excitation of a fluorophore and detection of a biomarker while minimizing spectral overlap of fluorescence emission. Antigens expressed at low levels should be detected with an antibody that is conjugated to a fluorophore with a robust emission fluorescence[67]. The recommended staining protocol was optimized for analysis on a cell sorter equipped with four lasers (405nm, 488nm, 561nm, 633nm) and 12 filters; however, filter configurations and laser availability vary between cytometers. To amend the protocol according to reagent and equipment availability, the reader is referred to additional resources, online spectrum viewers and published literature[67,68,69,70,71,72,73]. The multi-color staining protocol described herein requires compensation of spectral overlap to ensure that the sorted cell populations are GCBCs rather than inaccurate detection

Copyright © 2021 JoVE Creative Commons Attribution-NonCommercial-NoDerivs 3.0 Unported License

of fluorescence emission. B220 serves as a useful staining control for the described FACS (**Table 1B**) because PPs will have distinctive B220 negative and positive populations (**Figure 3C**), which allows for appropriate compensation of spectral overlap. The gating strategy presented in **Figure 3C** should be used as a guideline. The flow cytometry plots may vary depending on the staining conditions and cytometer settings. Nevertheless, 4-10% of the live cells should be $B220^{+}PNA^{HI}$ [35, 52].

All mutations within the JH4 intron of PP GCBCs must be validated to ensure that the observed mutations are truly reflective of SHM and not an artefact of PCR or sequencing. *AID*$^{-/-}$ B cells can serve as a useful negative control when examining the SHM phenotype in other mutant mouse models because these cells cannot complete SHM[17, 19]. The JH4 intron mutation rate in the of *AID*$^{-/-}$ GCBCs ($1.66x10^{-5}$ mutations/bp)[20, 21, 36, 37, 38, 50, 74] is comparable to the error rate of the high fidelity polymerase ($5.3x10^{-7}$ sub/base/doubling)[51, 52] that is used to amplify the DNA in the nested PCR. If *AID*$^{-/-}$ mice are not available, compare the observed mutation pattern and frequency to the published literature. Ig V regions accumulate 10^{-3}-10^{-4} mutations per base pair division, which is approximately 10^{6}-fold higher than the mutation rate of other gene loci[73, 75]. Results may vary with the age of the animal[76]. Alternatively, $B220^{+}PNA^{LO}$ cells, which marks non-GCBCs, may be used as a negative control in the absence of *AID*$^{-/-}$ mice[52]. If the mutation frequency in WT GCBCs is lower than expected, the WT germline JH4 intronic sequence may be disproportionately represented. In this case, ensure that GCBCs were stained and sorted appropriately and PCRs are free from WT germline JH4 intron contamination. Additionally, raw sequencing data in electropherograms should be analyzed thoroughly to ensure that mutations in the sequence text data are not artefacts of sequencing errors. For example, poor Sanger sequencing results may reduce the reliability of the sequence data (**Figure 4**). This quality control of the Sanger sequence data will increase the accuracy and reproducibility of the JH4 intron mutation analysis.

Disclosures

The authors have nothing to disclose.

Acknowledgments

We thank Tasuku Honjo for the *AID*$^{-/-}$ mice. This work was supported by The National Institute on Minority Health and Health Disparities (5G12MD007603), The National Cancer Institute (2U54CA132378), and The National Institute of General Medical Sciences (1SC1GM132035-01).

References

1. Murphy, K., Weaver, C. Janeway's Immunobiology. *Garland science.* (2016).
2. Alt, F. W. et al. VDJ recombination. *Immunology Today.* **13** (8), 306-314 (1992).
3. Schatz, D. G., Ji, Y. Recombination centres and the orchestration of V (D) J recombination. *Nature Reviews Immunology.* **11** (4), 251-263 (2011).
4. Oettinger, M. A., Schatz, D. G., Gorka, C., Baltimore, D. RAG-1 and RAG-2, adjacent genes that synergistically activate V (D) J recombination. *Science.* **248** (4962), 1517-1523 (1990).
5. Berek, C., Berger, A., Apel, M. Maturation of the immune response in germinal centers. *Cell.* **67** (6), 1121-1129 (1991).

Copyright © 2021 JoVE Creative Commons Attribution-NonCommercial-NoDerivs 3.0 Unported License

6. Linterman, M. A. et al. Foxp3+ follicular regulatory T cells control the germinal center response. *Nature Medicine.* **17** (8), 975 (2011).
7. Shulman, Z. et al. T follicular helper cell dynamics in germinal centers. *Science.* **341** (6146), 673-677 (2013).
8. Good-Jacobson, K. L. et al. PD-1 regulates germinal center B cell survival and the formation and affinity of long-lived plasma cells. *Nature Immunology.* **11** (6), 535 (2010).
9. Kerfoot, S. M. et al. Germinal center B cell and T follicular helper cell development initiates in the interfollicular zone. *Immunity.* **34** (6), 947-960 (2011).
10. Chaudhuri, J., Alt, F. W. Class-switch recombination: interplay of transcription, DNA deamination and DNA repair. *Nature Reviews Immunology.* **4** (7), 541-552 (2004).
11. Alt, F. W., Zhang, Y., Meng, F.L., Guo, C., Schwer, B. Mechanisms of programmed DNA lesions and genomic instability in the immune system. *Cell.* **152** (3), 417-429 (2013).
12. Xu, Z., Zan, H., Pone, E. J., Mai, T., Casali, P. Immunoglobulin class-switch DNA recombination: induction, targeting and beyond. *Nature Reviews Immunology.* **12** (7), 517-531 (2012).
13. Di Noia, J. M., Neuberger, M. S. Molecular mechanisms of antibody somatic hypermutation. *Annual Reviews of Biochemistry.* **76**, 1-22 (2007).
14. Peled, J. U. et al. The biochemistry of somatic hypermutation. *Annual Review of Immunology.* **26**, 481-511 (2008).
15. Liu, M., Schatz, D. G. Balancing AID and DNA repair during somatic hypermutation. *Trends in Immunology.* **30** (4), 173-181 (2009).
16. Methot, S., Di Noia, J. Molecular Mechanisms of Somatic Hypermutation and Class Switch Recombination. *Advances in Immunology.* **133**, 37-87 (2017).
17. Muramatsu, M. et al. Class switch recombination and hypermutation require activation-induced cytidine deaminase (AID), a potential RNA editing enzyme. *Cell.* **102** (5), 553-563 (2000).
18. Petersen-Mahrt, S. K., Harris, R. S., Neuberger, M. S. AID mutates E. coli suggesting a DNA deamination mechanism for antibody diversification. *Nature.* **418** (6893), 99 (2002).
19. Revy, P. et al. Activation-induced cytidine deaminase (AID) deficiency causes the autosomal recessive form of the Hyper-IgM syndrome (HIGM2). *Cell.* **102** (5), 565-575 (2000).
20. Petersen-Mahrt, S. DNA deamination in immunity. *Immunological Reviews.* **203** (1), 80-97 (2005).
21. Rada, C., Di Noia, J. M., Neuberger, M. S. Mismatch recognition and uracil excision provide complementary paths to both Ig switching and the A/T-focused phase of somatic mutation. *Molecular Cell.* **16** (2), 163-171 (2004).
22. Rada, C. et al. Immunoglobulin isotype switching is inhibited and somatic hypermutation perturbed in UNG-deficient mice. *Current Biology.* **12** (20), 1748-1755 (2002).
23. Schrader, C. E., Vardo, J., Stavnezer, J. Role for mismatch repair proteins Msh2, Mlh1, and Pms2 in immunoglobulin class switching shown by sequence

Copyright © 2021 JoVE Creative Commons Attribution-NonCommercial-NoDerivs 3.0 Unported License

analysis of recombination junctions. *The Journal of Experimental Medicine.* **195** (3), 367-373 (2002).

24. Martin, A. et al. Msh2 ATPase activity is essential for somatic hypermutation at AT basepairs and for efficient class switch recombination. *The Journal of Experimental Medicine.* **198** (8), 1171-1178 (2003).
25. Imai, K. et al. Human uracil–DNA glycosylase deficiency associated with profoundly impaired immunoglobulin class-switch recombination. *Nature Immunology.* **4** (10), 1023-1028 (2003).
26. Masani, S., Han, L., Yu, K. Apurinic/apyrimidinic endonuclease 1 is the essential nuclease during immunoglobulin class switch recombination. *Molecular and Cellular Biology.* **33** (7), 1468-1473 (2013).
27. Guikema, J. E. et al. APE1-and APE2-dependent DNA breaks in immunoglobulin class switch recombination. *The Journal of Experimental Medicine.* **204** (12), 3017-3026 (2007).
28. Schrader, C. E., Guikema, J. E., Wu, X., Stavnezer, J. The roles of APE1, APE2, DNA polymerase β and mismatch repair in creating S region DNA breaks during antibody class switch. *Philosophical Transactions of the Royal Society B: Biological Sciences.* **364** (1517), 645-652 (2009).
29. Roa, S. et al. MSH2/MSH6 complex promotes error-free repair of AID-induced dU: G mispairs as well as error-prone hypermutation of A: T sites. *PLoS One.* **5** (6), e11182 (2010).
30. Delbos, F., Aoufouchi, S., Faili, A., Weill, J.C., Reynaud, C.A. DNA polymerase η is the sole contributor of A/T modifications during immunoglobulin gene hypermutation in the mouse. *The Journal of Experimental Medicine.* **204** (1), 17-23 (2007).
31. Maul, R. W., Gearhart, P. J. AID and somatic hypermutation. *Advances in Immunology.* **105**, 159-191 (2010).
32. Shen, H. M., Tanaka, A., Bozek, G., Nicolae, D., Storb, U. Somatic hypermutation and class switch recombination in Msh6−/− Ung−/− double-knockout mice. *The Journal of Immunology.* **177** (8), 5386-5392 (2006).
33. Cheng, H.L. et al. Integrity of the AID serine-38 phosphorylation site is critical for class switch recombination and somatic hypermutation in mice. *Proceedings of the National Academy of Sciences.* **106** (8), 2717-2722 (2009).
34. Lebecque, S. G., Gearhart, P. J. Boundaries of somatic mutation in rearranged immunoglobulin genes: 5'boundary is near the promoter, and 3'boundary is approximately 1 kb from V (D) J gene. *The Journal of Experimental Medicine.* **172** (6), 1717-1727 (1990).
35. Jolly, C. J., Klix, N., Neuberger, M. S. Rapid methods for the analysis of immunoglobulin gene hypermutation: application to transgenic and gene targeted mice. *Nucleic Acids Research.* **25** (10), 1913-1919 (1997).
36. Choi, J. E., Matthews, A. J., Michel, G., Vuong, B. Q. AID Phosphorylation Regulates Mismatch Repair–Dependent Class Switch Recombination and Affinity Maturation. *The Journal of Immunology.* **204** (1), 13-22 (2020).
37. McBride, K. M. et al. Regulation of class switch recombination and somatic mutation by AID phosphorylation. *The Journal of Experimental Medicine.* **205** (11), 2585-2594 (2008).

Copyright © 2021 JoVE Creative Commons Attribution-NonCommercial-NoDerivs 3.0 Unported License

38. Liu, M. et al. Two levels of protection for the B cell genome during somatic hypermutation. *Nature.* **451** (7180), 841-845 (2008).

39. Ross, M., Birbeck, M., Wills, V., Forrester, J., Davis, A. Peanut lectin binding properties of germinal centers of mouse lymphoid tissues. *Nature.* **284**, 364-366 (1980).

40. Zhang, J., MacLennan, I. C., Liu, Y.J., Lane, P. J. Is rapid proliferation in B centroblasts linked to somatic mutation in memory B cell clones? *Immunology Letters.* 18 (4), 297-299, (1988).

41. Nieuwenhuis, P., Opstelten, D. Functional anatomy of germinal centers. *American Journal of Anatomy.* **170** (3), 421-435 (1984).

42. Lau, A. W., Brink, R. Selection in the germinal center. *Current Opinion in Immunology.* **63**, 29-34 (2020).

43. Victora, G. D., Nussenzweig, M. C. Germinal centers. *Annual Review of Immunology.* **30**, 429-457 (2012).

44. Mesin, L., Ersching, J., Victora, G. D. Germinal center B cell dynamics. *Immunity.* **45** (3), 471-482 (2016).

45. Reichert, R. A., Gallatin, W. M., Weissman, I. L., Butcher, E. C. Germinal center B cells lack homing receptors necessary for normal lymphocyte recirculation. *The Journal of Experimental Medicine.* **157** (3), 813-827 (1983).

46. Rose, M., Birbeck, M., Wills, V., Forrester, J., Davis, A. Peanut lectin binding properties of germinal centers of mouse lymphoid tissues. *Nature.* **284**, 364-366 (1980).

47. Hamada, S., Fujita, S. DAPI staining improved for quantitative cytofluorometry. *Histochemistry.* **79** (2), 219-226 (1983).

48. Otto, F. DAPI staining of fixed cells for high-resolution flow cytometry of nuclear DNA. *Methods in Cell Biology.* **33**, 105-110 (1990).

49. Butcher, E. et al. Surface phenotype of Peyer's patch germinal center cells: implications for the role of germinal centers in B cell differentiation. *The Journal of Immunology.* **129** (6), 2698-2707 (1982).

50. Rogerson, B. J., Harris, D. P., Swain, S. L., Burgess, D. O. Germinal center B cells in Peyer's patches of aged mice exhibit a normal activation phenotype and highly mutated IgM genes. *Mechanisms of Ageing and Development.* **124** (2), 155-165 (2003).

51. Potapov, V., Ong, J. L. Examining sources of error in PCR by single-molecule sequencing. *PloS One.* **12** (1), e0169774 (2017).

52. Gonzalez-Fernandez, A., Milstein, C. Analysis of somatic hypermutation in mouse Peyer's patches using immunoglobulin kappa light-chain transgenes. *Proceedings of the National Academy of Sciences.* **90** (21), 9862-9866 (1993).

53. Reboldi, A., Cyster, J. G. Peyer's patches: organizing B-cell responses at the intestinal frontier. *Immunological Reviews.* **271** (1), 230-245 (2016).

54. Betz, A. G., Rada, C., Pannell, R., Milstein, C., Neuberger, M. S. Passenger transgenes reveal intrinsic specificity of the antibody hypermutation mechanism: clustering, polarity, and specific hot spots. *Proceedings of the National Academy of Sciences.* **90** (6), 2385-2388 (1993).

55. Rada, C., Gupta, S. K., Gherardi, E., Milstein, C. Mutation and selection during the secondary response to 2-

Copyright © 2021 JoVE Creative Commons Attribution-NonCommercial-NoDerivs 3.0 Unported License

phenyloxazolone. *Proceedings of the National Academy of Sciences.* **88** (13), 5508-5512 (1991).

56. Heise, N., Klein, U. Somatic Hypermutation and Affinity Maturation Analysis Using the 4-Hydroxy-3-Nitrophenyl-Acetyl (NP) System. *Methods in Molecular Biology.* **1623**, 191-208 (2017).
57. Smith, F., Cumano, A., Licht, A., Pecht, I., Rajewsky, K. Low affinity of kappa chain bearing (4-hydroxy-3-nitrophenyl) acetyl (NP)-specific antibodies in the primary antibody repertoire of C57BL/6 mice may explain lambda chain dominance in primary anti-NP responses. *Molecular Immunology.* **22** (10), 1209-1216 (1985).
58. Takahashi, Y., Dutta, P. R., Cerasoli, D. M., Kelsoe, G. In situ studies of the primary immune response to (4-hydroxy-3-nitrophenyl) acetyl. V. Affinity maturation develops in two stages of clonal selection. *The Journal of Experimental Medicine.* **187** (6), 885-895 (1998).
59. Allen, D., Simon, T., Sablitzky, F., Rajewsky, K., Cumano, A. Antibody engineering for the analysis of affinity maturation of an anti-hapten response. *The EMBO Journal.* **7** (7), 1995-2001 (1988).
60. Cumano, A., Rajewsky, K. Clonal recruitment and somatic mutation in the generation of immunological memory to the hapten NP. *The EMBO Journal.* **5** (10), 2459-2468 (1986).
61. Smith, K., Nossal, G., Tarlinton, D. M. FAS is highly expressed in the germinal center but is not required for regulation of the B-cell response to antigen. *Proceedings of the National Academy of Sciences.* **92** (25), 11628-11632 (1995).
62. Hao, Z. et al. Fas receptor expression in germinal-center B cells is essential for T and B lymphocyte homeostasis. *Immunity.* **29** (4), 615-627 (2008).
63. Cervenak, L., Magyar, A., Boja, R., László, G. Differential expression of GL7 activation antigen on bone marrow B cell subpopulations and peripheral B cells. *Immunology Letters.* **78** (2), 89-96 (2001).
64. Naito, Y. et al. Germinal center marker GL7 probes activation-dependent repression of N-glycolylneuraminic acid, a sialic acid species involved in the negative modulation of B-cell activation. *Molecular and Cellular Biology.* **27** (8), 3008-3022 (2007).
65. Olson, W. J. et al. Orphan Nuclear Receptor NR2F6 Suppresses T Follicular Helper Cell Accumulation through Regulation of IL-21. *Cell Reports.* **28** (11), 2878-2891 (2019).
66. Dorsett, Y. et al. MicroRNA-155 suppresses activation-induced cytidine deaminase-mediated Myc-Igh translocation. *Immunity.* **28** (5), 630-638 (2008).
67. Goetz, C., Hammerbeck, C., Bonnevier, J. Flow Cytometry Basics for the Non-Expert. *Springer.* (2018).
68. Hawley, T. S., Herbert, D. J., Eaker, S. S., Hawley, R. G. Flow Cytometry Protocols. *Springer.* (2004).
69. Costa, E. et al. A new automated flow cytometry data analysis approach for the diagnostic screening of neoplastic B-cell disorders in peripheral blood samples with absolute lymphocytosis. *Leukemia.* **20** (7), 1221-1230 (2006).
70. McKinnon, K. M. Flow cytometry: An overview. *Current Protocols in Immunology.* **120** (1), 5.1.1-5.1.11 (2018).
71. McKinnon, K. M. Multiparameter Conventional Flow Cytometry. *Methods in Molecular Biology.* 1678, 139-150 (2018).
72. Lucchesi, S. et al. Computational Analysis of Multiparametric Flow Cytometric Data to Dissect B Cell

Copyright © 2021 JoVE Creative Commons Attribution-NonCommercial-NoDerivs 3.0 Unported License

Subsets in Vaccine Studies. *Cytometry Part A.* **97**, 259-267 (2019).

73. Longerich, S., Tanaka, A., Bozek, G., Nicolae, D., Storb, U. The very 5′ end and the constant region of Ig genes are spared from somatic mutation because AID does not access these regions. *The Journal of Experimental Medicine.* **202** (10), 1443-1454 (2005).
74. Retter, I. et al. Sequence and characterization of the Ig heavy chain constant and partial variable region of the mouse strain 129S1. *The Journal of Immunology.* **179** (4), 2419-2427 (2007).
75. Shen, H. M., Peters, A., Baron, B., Zhu, X., Storb, U. Mutation of BCL-6 gene in normal B cells by the process of somatic hypermutation of Ig genes. *Science.* **280** (5370), 1750-1752 (1998).
76. Richter, K. et al. Altered pattern of immunoglobulin hypermutation in mice deficient in Slip-GC protein. *Journal of Biological Chemistry.* **287** (38), 31856-31865 (2012).

Copyright © 2021 JoVE Creative Commons Attribution-NonCommercial-NoDerivs 3.0 Unported License